

Review of formal methodologies for wind–slope correction of wildfire rate of spread

Jason J. Sharples

School of Physical, Environmental and Mathematical Sciences, UNSW@ADFA, Canberra, ACT 2600, Australia; and Bushfire Cooperative Research Centre, Level 5, 340 Albert St, East Melbourne, VIC 3002, Australia. Email: j.sharples@adfa.edu.au

Abstract. The effects of wind and topographic slope are important considerations when determining the rate and direction of spread of wildfires. Accordingly, most models used to predict the direction and rate of spread contain components designed to account for these effects. Over the years, a variety of different approaches have been developed. In the present manuscript, we examine the various mathematical models employed to account for the effects of wind and slope at a formal level, making comparisons where appropriate. The methods reviewed include scalar methods, which ignore the directional nature of wind and slope effects, as well as methods in which the effects of wind and slope are combined in a vectorial manner. Both empirical and physical models for wind–slope correction are considered.

Introduction

Research into wildland fires over the last 50–60 years has identified wind and terrain as two of the chief factors determining the severity and rate of spread of a fire (Fons 1946; Byram 1959; Byram *et al.* 1966; McArthur 1967; Weise 1993; Nelson 2002; Viegas 2004a; Linn *et al.* 2007). Wind has the effect of tilting the flames forward, over and onto unburnt fuel, extending the pre-heating range and thus leading to more intense fire behaviour and greater rates of spread. The slope of the terrain has a similar effect, by essentially bringing the ground, and hence the fuel on it, into closer proximity to the flames. Under typical conditions, fires propagating upslope with the wind exhibit the greatest rates of spread, whereas fires travelling downslope against the wind exhibit the lowest rates of spread. Consequently, the majority of fire spread models in operational use today contain a component that attempts to modify fire spread rates by applying a factor that emulates the combined effects of wind and topographic slope.

In the wake of the disastrous bushfires over the high country of south-eastern Australia during January 2003, there has been renewed interest in the interaction of wind and terrain and their effect on fire behaviour. Evidence arising from the 2003 fires suggests that the interaction of weather (particularly wind) and terrain played a crucial role in escalating the fire to the level that impacted on Canberra suburbs. The 1994 South Canyon fire on Storm King Mountain, Colorado, during which 14 fire-fighters tragically lost their lives, serves as another example of the importance of understanding the interaction of wind and terrain (Butler *et al.* 1998, 2003), as do other blow-up fires such as the Butte Fire of 1985 (Rothermel and Mutch 1986) and the Mann Gulch Fire of 1949 (Rothermel 1993). Terrain–wind interactions such as dynamic channelling, coupled with low fuel moisture content, can result in massive expansion of the flanks of a fire and the generation of severe ember storms (McRae 2004b; Dold *et al.* 2005; McRae *et al.* 2006). Although it is important not to underestimate the role that additional factors, such as fuel properties and

fire–atmosphere–terrain interactions, play in these types of blow-up conditions, it is worthwhile to examine the way that wind and terrain parameters such as topographic slope and aspect enter into fire propagation models. Indeed, because the combined effects of wind and topographic slope form a major component of general terrain–weather interactions, a valuable first step is to quantitatively review the different methods employed in accounting for these effects in existing point–functional models.

We use the term ‘point–functional models’ as in Linn *et al.* (2007) to describe models that use information about wind and terrain at a particular point location to calculate rate and direction of fire spread at that location. Classifying these models as such distinguishes them from the more computationally intensive coupled transport models (e.g. Linn 1997; Forthofer *et al.* 2003; Butler *et al.* 2006; Linn *et al.* 2007). Linn *et al.* (2007) provide examples of situations in which local information on wind and terrain factors should produce good fire spread predictions and situations where it should not. Hence, although wind and slope correction methods can improve the predictive capability of point–functional models of fire spread, their inclusion does not necessarily overcome all of the limitations of these models. This disadvantage, however, is balanced by the fact that point–functional models are more intuitive and numerically inexpensive, when compared with coupled transport models.

Weise and Biging (1997) give a qualitative comparison of several point–functional fire spread models that incorporate wind and slope effects and compare their predictions with experimental data. The focus of the present manuscript is thus not to compare the quality of prediction of various fire spread models incorporating wind and slope effects; rather, it compares the particular components of the models pertaining to wind and slope effects at a formal level. We present a detailed review of the formal wind–slope correction methods used in a suite of fire spread models, some of which were developed after the publication of Weise and Biging (1997). The present manuscript then

serves as a continuation of the work of Weise and Biging, as well as a companion paper that hopefully elucidates some of the mathematical details. The methods considered here are those of McArthur (McArthur 1966, 1967; Noble *et al.* 1980), Rothermel and Albini (Rothermel 1972; Albini 1976), Finney (1998), McAlpine *et al.* (1991), Nelson (2002), McRae (2004a), Pagni and Peterson (1973), and Morandini *et al.* (2002).

It is important to note that in each of the methods discussed in the following sections, it is implicitly assumed that a given set of wind and slope conditions uniquely defines the corresponding rate and direction of spread of a fire. In making this assumption, we are ignoring dynamic feedback effects and fire–atmosphere–terrain coupling, which, in the general case, mean that the rate and direction of spread of a fire cannot be univocally defined in terms of the wind and slope conditions (Viegas and Pita 2004; Viegas 2004a, 2006; Linn *et al.* 2007). Similarly, we are also ignoring transverse convective effects along the fireline that can cause dynamic fire behaviour, even when wind and slope conditions are unchanging (Viegas 2002; Oliveras *et al.* 2006).

Notation and conventions

Central to the idea of wind–slope correction of fire spread rates are the notions of wind vector, topographic slope and topographic aspect, which we now formally define.

The direction and speed at which a fire propagates are largely determined by the wind direction and speed. These two quantities make up a wind vector, which we denote by \mathbf{w} . The wind speed may then be denoted as $\|\mathbf{w}\|$ while the wind direction will be denoted by the angle θ_w . However, owing to the convention that wind direction is given in terms of where the wind is coming from rather than where it is heading, the wind vector points in the $\theta_w + \pi$ direction, expressing angles in radians ($\pi = 180^\circ$). This means that the direction of fire spread (in flat terrain) will be opposite to the wind direction (e.g. a westerly wind will propagate a fire towards the east).

Topographic slope is the maximum inclination of a terrain surface at a particular point. Given an elevation function $h(x,y)$, where x and y denote the horizontal quantifiers of position, e.g. longitude and latitude, the topographic slope at a point is formally defined as the length of the gradient vector field. Recall that the gradient vector field is given by

$$\nabla h(x,y) = \left(\frac{\partial h}{\partial x}, \frac{\partial h}{\partial y} \right)$$

and thus has length

$$\|\nabla h\| = \sqrt{\left(\frac{\partial h}{\partial x} \right)^2 + \left(\frac{\partial h}{\partial y} \right)^2}$$

Topographic slope is typically described by the topographic slope angle, which we denote as γ_s . We note that $\|\nabla h\| = \tan \gamma_s$.

The alignment of topographic slope is known as topographic aspect. To formally define topographic aspect, consider an outward pointing vector that is normal to the terrain surface at some given point. This normal vector can be decomposed into two components, the horizontal component, which lies in the horizontal xy -plane, and the vertical component, which is perpendicular to the xy -plane. The direction of the horizontal

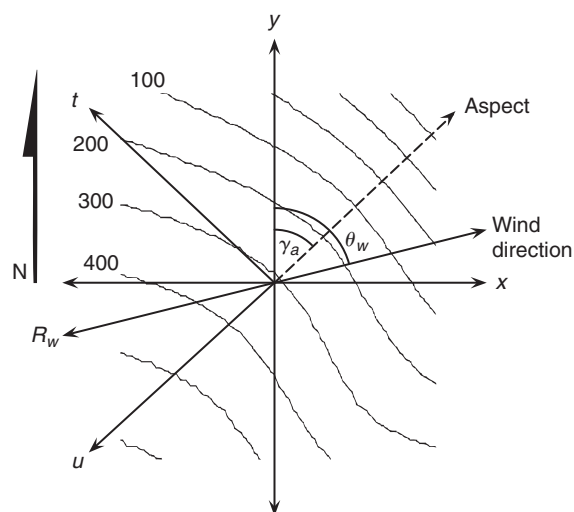


Fig. 1. Schematic depicting the relationship between the cardinal and terrain-following coordinates and the terrain surface contours.

component of the normal vector defines the topographic aspect, which is expressed in terms of the angle between this direction and due north. We note that the aspect direction points down-slope. Given an elevation function $h(x,y)$, which represents the topography, the topographic aspect can be equivalently defined as the direction of the negative gradient vector field $-\nabla h(x,y)$. We denote topographic aspect by the angle γ_a . Note that if the wind direction and topographic aspect are in alignment, with the wind flowing upslope, then $\gamma_a = \theta_w$, whereas for wind flowing directly downslope, $\gamma_a = \theta_w + \pi$ (expressing angles in radians).

It is important to note that the conventions associated with the cardinal compass directions, in which angles increase in the clockwise direction (left-handed coordinate system), are at odds with the usual algebraic convention in which angles increase in the anticlockwise direction (right-handed coordinate system). As applications are employed in operational environments that typically deal with directions as determined by compass, we shall adopt the left-handed coordinate system throughout. This means that sine and cosine functions will appear in reverse order to what can be expected in a basic algebra textbook.

We will often find it convenient to work in *terrain-following* coordinates that align with the upslope and across-slope (transverse) directions. To distinguish these coordinates from the standard coordinates aligned with the cardinal directions, we make the following definitions. Standard coordinates are defined with respect to the $\{x,y\}$ coordinate frame, where the positive y -axis is aligned with due north and the positive x -axis is aligned in the easterly direction. Local (terrain-following) coordinates are defined at each point on the terrain surface with respect to the $\{t,u\}$ coordinate frame, where the positive u -axis points in the upslope direction and the positive t -axis points in the transverse direction, to the right of the positive u -axis. Fig. 1 illustrates the relation between the two coordinate systems and a terrain surface. We will use the notation \hat{y} , \hat{u} , etc. to denote, respectively, the unit vectors in the directions of y , u , etc.

We also make the distinction between the base, or no-wind, rate of spread and the wind-induced rate of spread of a fire.

The base rate of spread is the rate of spread of a fire through a particular fuel under conditions of no wind and no slope. The wind-induced rate of spread is the rate of spread of the fire through a particular fuel under windy conditions but in the absence of slope. In the current paper, both the base and wind-induced rates of spread will be assumed to be given as some function of the relevant meteorological variables and fuel properties. Relevant variables for the base rate of spread include temperature, rainfall and humidity, and fuel properties such as moisture content and flammability. Relevant variables for the wind-induced rate of spread would also include wind speed and direction. In what follows, we will use R_0 to denote the base rate of spread and R_w to denote the wind-induced rate of spread.

To incorporate the combined effects of wind and slope in models of fire spread, two general approaches are commonly employed. The first approach assumes the base rate of spread as given and calculates a wind-slope correction factor. This factor is then used to modify the base rate of spread to give a rate of spread that incorporates the effects of wind and slope (Rothermel 1972; Albini 1976; McAlpine *et al.* 1991; Santoni *et al.* 1999; Morandini *et al.* 2002). In the second approach, a slope correction factor is calculated. The wind- and slope-affected rate of spread is then given by this factor multiplied by the wind-induced rate of spread (McArthur 1966, 1967; Noble *et al.* 1980; McRae 2004a).

Wind-slope correction methods

McArthur

McArthur's fire danger meters form the basis for fire danger forecasting and for understanding fire behaviour in Australia (McArthur 1966). The meters have been converted into equations for more convenient use in computer applications (Noble *et al.* 1980). The equations allow calculation of the wind-induced rate of spread of a fire using standard meteorological variables and measures of drought factor or grass curing as inputs. The direction of the wind-induced rate of spread is taken to be opposite to the wind direction.

For a fire propagating in sloping terrain, this wind-induced rate of spread is amended as

$$R(w, \gamma_s) = R_w \exp(0.069\gamma_s) \quad (1)$$

where γ_s is the slope of the terrain expressed in degrees. Eqn 1 embodies the observation that a fire's rate of spread approximately doubles for every 10° increase in topographic slope (it halves for a 10° decrease in slope).

It is important to note that some fire spread models in use in Australia that do not employ the McArthur fire spread model still use Eqn 1 to adjust for slope effects. Examples of such models are the Western Australian 'Red Book' (Sneeuwjagt and Peet 1985; Beck 1990) and the FIRESCAPE model (McCarthy and Cary 2002).

Strictly speaking, Eqn 1 is a scalar equation and as such only applies to a fire travelling directly upslope (or downslope), which is to say that it only applies when the wind direction is directly upslope or downslope. In reality, however, both wind and slope act in combination to alter the speed and direction that a fire will spread, and at any given site it is unlikely that these two factors will be in alignment. Consequently, a fire at a given site

will generally not be travelling directly upslope (or downslope). When this is the case, Eqn 1 will not directly apply.

To obtain a more generally applicable expression, it is convenient to treat a fire's rate of spread and its direction of propagation as a single rate of spread vector \mathbf{R} . Thus at any given point on the fire front, the vector \mathbf{R} has length equal to the scalar rate of spread R and points in the direction that the fire is propagating. We may proceed in at least two ways:

1. Scalar method: we can use Eqn 1, replacing the topographic slope γ_s with the slope experienced in the direction that the fire is propagating, to obtain a slope-corrected scalar rate of spread; or
2. Vector method: we can vectorially decompose the wind-induced rate of spread vector into components that point upslope and across-slope, apply Eqn 1 to the upslope component and then recombine the amended components to obtain a slope-corrected rate of spread vector.

Proceeding the first way, we are required to calculate the effective slope experienced in the direction of the wind-induced rate of spread vector \mathbf{R}_w . If we let the effective slope angle be ψ , then $\tan \psi$ is given by the directional derivative (Stewart 1991) of the terrain surface in the direction of the wind-induced rate of spread vector. We assume that the terrain surface is given as the graph of some elevation function $h(x,y)$. To calculate $\tan \psi$ at a point on the terrain surface, it is useful to use the terrain-following coordinates defined in the *Notation and conventions* section. The unit vector in the direction of \mathbf{R}_w , denoted $\hat{\mathbf{R}}_w$, expressed in this coordinate system is given by

$$\hat{\mathbf{R}}_w = \sin(\theta_w - \gamma_a)\hat{\mathbf{t}} + \cos(\theta_w - \gamma_a)\hat{\mathbf{u}} \quad (2)$$

where $\hat{\mathbf{t}}$ and $\hat{\mathbf{u}}$ are the unit vectors in the positive t and u directions. The directional derivative of the terrain surface h in the direction of $\hat{\mathbf{R}}_w$ is defined by (Stewart 1991) and is given by

$$D_{\hat{\mathbf{R}}_w} h = \nabla h \cdot \hat{\mathbf{R}}_w \quad (3)$$

Thus, calculating in local coordinates, we have

$$\begin{aligned} \tan \psi &= D_{\hat{\mathbf{R}}_w} h \\ &= \nabla h \cdot \hat{\mathbf{R}}_w \\ &= \left(\frac{\partial h}{\partial t} \hat{\mathbf{t}} + \frac{\partial h}{\partial u} \hat{\mathbf{u}} \right) \cdot (\sin(\theta_w - \gamma_a)\hat{\mathbf{t}} + \cos(\theta_w - \gamma_a)\hat{\mathbf{u}}) \\ &= \frac{\partial h}{\partial t} \sin(\theta_w - \gamma_a) + \frac{\partial h}{\partial u} \cos(\theta_w - \gamma_a) \end{aligned}$$

Recall at this point that we arranged our coordinate axes so that the \mathbf{t} -axis aligned with the transverse direction. This means that the \mathbf{t} -axis follows lines of constant elevation and so

$$\frac{\partial h}{\partial t} = 0$$

Similarly, the \mathbf{u} -axis is aligned with the upslope direction and so

$$\frac{\partial h}{\partial u} = \tan \gamma_s$$

Hence

$$\tan \psi = \tan \gamma_s \cos(\theta_w - \gamma_a) \quad (4)$$

Therefore the slope-corrected rate of spread, according to this method, is given by

$$R(w, \gamma_s) = R_w \exp(0.069 \tan^{-1}(\tan \gamma_s \cos(\theta_w - \gamma_a))) \quad (5)$$

Note that Eqn 5 is a scalar equation – only the magnitude of the rate of spread vector has been affected; the direction of the slope-corrected rate of spread must still be taken as the direction of the wind-induced rate of spread vector. Eqn 5 has been employed in fire spread models such as FIRESCAPE (G. J. Cary, pers. comm., 2006).

Proceeding the second way, we separate the wind-induced rate of spread vector into components, apply Eqn 1 to the upslope component and then recombine the amended components. Using the terrain-following coordinate system again, we may decompose \mathbf{R}_w as in Eqn 2.

The transverse component of \mathbf{R}_w experiences no topographic slope (as it follows lines of constant elevation) and so no slope correction is required for this component of \mathbf{R}_w . However, the upslope component of \mathbf{R}_w points directly upslope (or downslope), and so Eqn 1 can be applied. This results in a slope-corrected version of the upslope component of \mathbf{R}_w given by

$$R_w \cos(\theta_w - \gamma_a) \exp(0.069 \gamma_s) \hat{\mathbf{u}}$$

The unaltered transverse component can now be recombined with the corrected upslope component to give the slope-corrected rate of spread vector $\mathbf{R}(w, \gamma_s)$:

$$\mathbf{R}(w, \gamma_s) = R_w \sin(\theta_w - \gamma_a) \hat{\mathbf{t}} + R_w \cos(\theta_w - \gamma_a) \exp(0.069 \gamma_s) \hat{\mathbf{u}} \quad (6)$$

Note that the magnitude of the slope-corrected rate of spread vector is given by

$$R(w, \gamma_s) = R_w \sqrt{\sin^2(\theta_w - \gamma_a) + \cos^2(\theta_w - \gamma_a) \exp(0.138 \gamma_s)} \quad (7)$$

and that the direction of the slope-corrected rate of spread vector, relative to the cardinal axes, is given by

$$\theta_{\mathbf{R}} = \gamma_a + \frac{\pi}{2} + \tan^{-1}\{\cot(\theta_w - \gamma_a) \exp(0.069 \gamma_s)\} \quad (8)$$

Note that both the magnitude and the direction of the slope-corrected rate of spread will differ depending on whether we adopt the first or second procedure above. A comparison of the magnitude and direction of the slope-corrected rate of spread vectors calculated using the two procedures is shown in Fig. 2. The curves in Fig. 2 are derived assuming that the wind is blowing from the north and that the topographic slope is 20° . The interpretation of the curves in Fig. 2 is best explained through an example. Consider a fire driven by a northerly wind with a head-fire rate of spread of 1 km h^{-1} . In flat terrain, such a fire would tend to head in a southerly direction. The black curves in Fig. 2 suggest, however, that when such a fire experiences a topographic slope of 20° aligned with a topographic aspect of 45° , the fire will tend to head in a direction roughly 30° west of south ($\approx 210^\circ$) and will propagate with a speed of $\sim 2.9 \text{ km h}^{-1}$. Thus the effect of topographic slope accelerates the fire by a factor of three and deflects its direction of propagation by $\sim 30^\circ$ to the west.

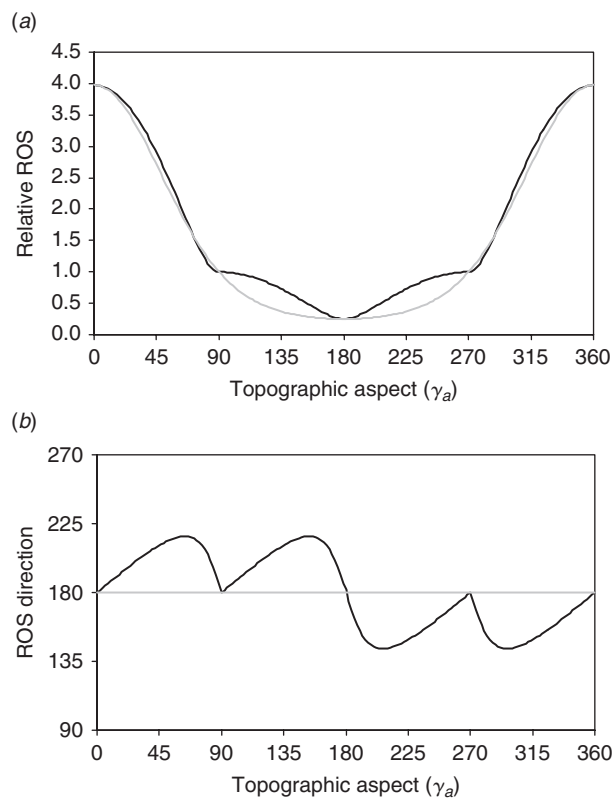


Fig. 2. (a) Magnitude of the slope-corrected rate of spread vector: the black line is derived using the vector method, whereas the grey line is derived using the scalar method; (b) direction of the slope-corrected rate of spread vector: the black line is derived using the vector method; the grey line indicates that the scalar method doesn't alter the direction of spread. A wind-induced rate of spread of 1 km h^{-1} and a topographic slope of 20° have been assumed.

The scalar and vector methods described in this section are only two of many possible methods that could be devised to combine wind and slope information within the McArthur framework. Another will be described below after discussing the method of McAlpine, whereas others still are being developed (K. Tolhurst and D. Chong, pers. comm., 2006).

Rothermel, Albini and Finney

Rothermel (1972) models the impact of wind and slope on a fire front as independent, additive factors ϕ_w and ϕ_s , respectively. The scalar rate of spread in the direction θ (measured from the upslope direction, i.e. $\gamma_a \pm \pi$) is then given by

$$R(\theta) = (1 + \phi_s(\theta) + \phi(\theta, \theta_w))R_0 \quad (9)$$

where R_0 is the corresponding rate of spread in the absence of wind and topographic slope. It is important to note that the inclusion of the parameter θ allows derivation of a wind-slope correction factor for all parts of the fire's perimeter, not just the head.

For that part of the fire front spreading in the direction that the wind is blowing ($\theta = \theta_w - \gamma_a$), the wind coefficient ϕ_w is estimated using a power law as

$$\phi_w^* = C \|\mathbf{w}\|^B \quad (10)$$

where the coefficients B and C are functions of fuel properties such as the packing ratio and particle size.

For the general case, when $\theta \neq \theta_w - \gamma_a$, we replace \mathbf{w} with the component of the wind vector parallel to the direction θ ; hence

$$\phi_w(\theta, \theta_w) = \phi_w^* \cos^B(\theta_w - \gamma_a - \theta) \quad (11)$$

or, more succinctly,

$$\phi_w(\theta, \theta_w) = C(\mathbf{w} \cdot \hat{\theta})^B \quad (12)$$

where $\hat{\theta} = \sin \theta \hat{\mathbf{t}} + \cos \theta \hat{\mathbf{u}}$ is the unit vector in the direction θ from uphill.

Beer (1991) and Weber (2001) point out that it is possible for the parameters B and C to exceed unity, in which case the model suggests that the fire can spread faster than the wind driving it. Although this is not a major concern for low wind speeds, as in the absence of wind a fire will still propagate at a non-zero rate owing to radiative effects, it can cause problems when a fire is driven by strong winds and advection of heated gases becomes the dominant influence on its propagation. In this case, the problems can be remedied by placing an upper limit on the value of ϕ_w .

For the case of a fire spreading directly upslope ($\theta = 0$), the slope coefficient is estimated as

$$\phi_s^* = A \tan^2 \gamma_s \quad (13)$$

where the coefficient A is a function of fuel particle size and packing ratio.

For the general case ($\theta \neq 0$), the slope coefficient $\phi_s(\theta)$ is based on the topographic slope sensed in the direction θ from upslope. It is given by (Albini 1976)

$$\phi_s(\theta) = A \tan^2 \gamma_s \cos^2 \theta = \phi_s^* \cos^2 \theta \quad (14)$$

Note here that when the elevation surface is given as the graph of a function $h(x,y)$, then we can also express Eqn 14 in more general terms as

$$\phi_s(\theta) = A(D_{\hat{\theta}}h)^2 = A(\nabla h \cdot \hat{\theta})^2 \quad (15)$$

The methods used to derive the general wind and slope correction factors above are similar to those employed in the scalar McArthur method. In essence, the quantities in Eqns 10 and 13, which govern the special case of fire spreading directly upslope under the influence of upslope winds, are simply replaced with the appropriate components of the slope and wind vectors in the general direction of interest.

For a wind blowing from the north, the relative rate of spread in the southerly direction is given by

$$1 + C\|\mathbf{w}\|^B \pm A \tan^2 \gamma_s \cos^2 \gamma_a \quad (16)$$

Here the positive sign applies when the aspect has a south-facing component; the negative sign applies when the aspect has a north-facing component.

Fig. 3 shows how the scalar rate of spread in the southerly direction varies with topographic aspect. The curves in Fig. 3 are derived assuming a topographic slope of 20° and a 10-km h^{-1}

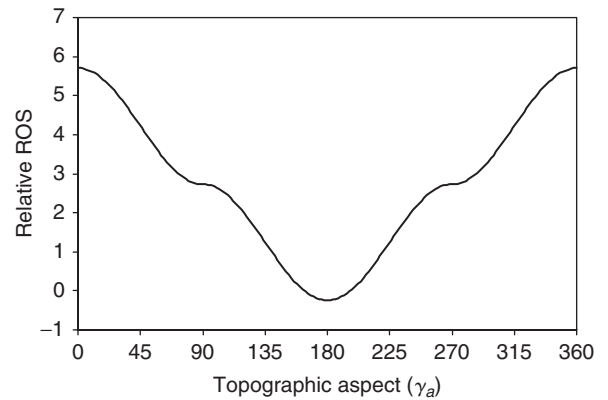


Fig. 3. Wind-slope correction factor for southerly fire spread according to the Rothermel-Albini method. A topographic slope of 20° and a wind blowing from the north at 10 km h^{-1} have been assumed.

wind blowing from the north. The constants were assumed to be as given in Weise and Biging (1997).

It is interesting to note that relative rate of spread predicted by the scalar method of Rothermel and Albini is of similar shape to that predicted by the vector McArthur method. The approach also allows the possibility of a fire burning upslope against the direction of the bulk winds, given that unburnt fuel is available to carry the fire in that direction. This can occur, for example, when a spot-fire ignites on a lee slope. This possibility is reflected in the negative relative rate of spread values in Fig. 3 for aspects that are approximately south-facing. According to this model, a fire will propagate upslope against northerly bulk winds whenever the aspect has a south-facing component and satisfies

$$\cos^2 \gamma_a > \frac{1 + C\|\mathbf{w}\|^B}{A \tan^2 \gamma_s} \quad (17)$$

For the example depicted in Fig. 3, the fire will propagate upslope against the wind for aspects in the range of 162° to 197° .

Finney (1998) extends the concepts of Rothermel and Albini discussed above to a full two-dimensional fire spread model called FARSITE using Huygens' Principle. In this method, the head-fire rate of spread is again given by Eqn 9. The orientation of the ellipses that form the basis for the application of Huygens' Principle, however, are given by combining the wind and slope coefficients (Eqns 10 and 13) using vector addition. The orientation of the ellipse at a point defines the direction of spread at that point. The direction of spread according to Finney (1998) is thus in the direction of the vector

$$\mathbf{U}_{ws} = C\|\mathbf{w}\|^B \sin(\theta_w - \gamma_a) \hat{\mathbf{t}} + \{C\|\mathbf{w}\|^B \cos(\theta_w - \gamma_a) + A \tan^2 \gamma_s\} \hat{\mathbf{u}} \quad (18)$$

This modification extends the scalar Rothermel model into a vector model for fire spread.

McAlpine

McAlpine *et al.* (1991) model the effects of wind and slope on fire behaviour within the context of the Canadian Forest Fire

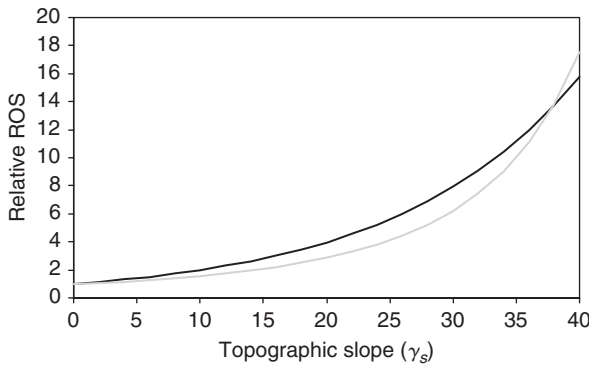


Fig. 4. Comparison of the slope-correction factors from the McArthur (black) and McAlpine (grey) methods.

Behaviour Prediction (FBP) System. This system utilises the Canadian Fire Weather Index (FWI) System, a component of which is the Initial Spread Index (*ISI*). The Initial Spread Index uses information on wind and fuel moisture to estimate the linear rate of spread of a head-fire. Topographic slope is not specifically included as an additional variable in this system. The *ISI* is given in terms of the wind vector \mathbf{w} and the fine fuel moisture content after drying m by (Van Wagner and Pickett 1975; Forestry Canada Fire Danger Group 1992)

$$ISI = 0.208 f(\mathbf{w})g(m) \quad (19)$$

where

$$f(\mathbf{w}) = \exp(0.05039\|\mathbf{w}\|) \quad (20)$$

and

$$g(m) = (91.9 \exp(-0.1386)) \left(1 + \frac{m^{5.31}}{4.93 \times 10^7}\right) \quad (21)$$

where m is derived from the fine fuel moisture content (FFMC) as (Forestry Canada Fire Danger Group 1992):

$$m = \frac{147.2(101 - \text{FFMC})}{59.5 + \text{FFMC}}$$

The rate of spread is then given by

$$R = \beta_0(1 - \exp(-\beta_1 ISI))^{\beta_2} \quad (22)$$

where β_0 , β_1 and β_2 are positive, fuel-specific constants.

To account for the effects of slope on a head-fire's rate of advance in the Canadian Fire Weather Index, McAlpine *et al.* (1991) present a method for converting the effect of slope into an equivalent wind speed and direction. Their approach is based on the equation

$$R_s = R_0 \exp(3.533(\tan \gamma_s)^{1.2}) \quad (23)$$

which was obtained by fitting a curve to a combination of spread rate data and model predictions taken from five separate studies concerned with accounting for the effect of topographic slope (Van Wagner 1977). One of the datasets used in fitting Eqn 23 was the one used to derive the McArthur model discussed above and thus it is not surprising to find that the functions on the right hand side of Eqns 1 and 23 agree quite closely up to slope angles of 40°. The two functions are shown in Fig. 4.

Eqn 23 can then be substituted into Eqn 22, which can be rearranged to give the initial spread index due to the effects of slope

$$ISI_s = -\frac{1}{\beta_1} \ln \left[1 - \left(\frac{R_s}{\beta_0} \right)^{\frac{1}{\beta_2}} \right] \quad (24)$$

Eqns 19 and 20 can be combined and rearranged to give an equation for wind speed in terms of *ISI* and m . Substituting the *ISI* due to slope, given by Eqn 24, into the resulting equation, we deduce an equivalent wind vector \mathbf{w}_s^* that mimics the effect of topographic slope. The magnitude of this vector, known as the wind speed equivalent, is given by

$$\|\mathbf{w}_s^*\| = 19.845 \ln \left\{ -\ln \left[1 - \left(\frac{R_0 \exp(3.533(\tan \gamma_s)^{1.2})}{\beta_0} \right)^{\frac{1}{\beta_2}} \right] \right\} - 19.845 \ln(0.208\beta_1 g(m)) \quad (25)$$

while its direction is taken as the upslope direction.

This equivalent wind vector, which accounts for slope effects, and the actual wind vector can then be added to produce a net effective wind vector $\mathbf{U}_{ws} = \mathbf{w} + \mathbf{w}_s^*$ that accounts for the combined effects of wind and slope. The net effective wind vector then substitutes for the actual wind vector in Eqn 20 when a topographic slope is present. Fig. 5 shows how the net effective wind speed and direction change as topographic aspect is varied. The curves in Fig. 5 were derived assuming a C-7 fuel type with an FFMC of 89% and a 10-km h⁻¹ wind blowing from the north. A C-7 fuel type corresponds to $\beta_0 = 45$, $\beta_1 = 0.0305$ and $\beta_2 = 2$. The light grey, black and dark grey curves correspond to topographic slopes of 10°, 20° and 30°, respectively.

The net effective wind direction curves in Fig. 5b exhibit different behaviour depending on whether $\|\mathbf{w}_s^*\| < \|\mathbf{w}\|$ or not, particularly for aspects that are approximately south-facing ($\gamma_a \approx 180^\circ$). If $\|\mathbf{w}_s^*\| < \|\mathbf{w}\|$, then the ambient wind will dominate an opposing upslope wind equivalent (e.g. the light grey curve in Fig. 5b), otherwise the model predicts that the fire will burn uphill against the wind on lee slopes (e.g. the black and dark grey curves in Fig. 5b).

A shortcoming of the approach of McAlpine *et al.* is that the wind speed equivalent is only defined when

$$R_0 \exp(3.533(\tan \gamma_s)^{1.2}) < \beta_0 \quad (26)$$

For the example portrayed in Fig. 5, this condition is violated when $\gamma_s \approx 50^\circ$.

We note that although the shapes of the curves describing the variation in effective wind speed are similar to relative rate of spread curves obtained using the McArthur method, the effective wind direction curves display significantly different behaviour to that seen in Fig. 2b. The cusp points seen at aspect angles of 50° and 270° in Fig. 2b are not present in Fig. 5b. In the method of McAlpine *et al.*, an upslope wind-equivalent vector is *added* to the upslope component of the actual wind vector before the result is added to the transverse component of the actual wind vector. In the McArthur vector method, the upslope component of the wind-induced rate of spread is *multiplied* by a scalar slope correction factor before being added to the transverse component of the wind-induced rate of spread. However, when $\gamma_a \approx 90^\circ$ or

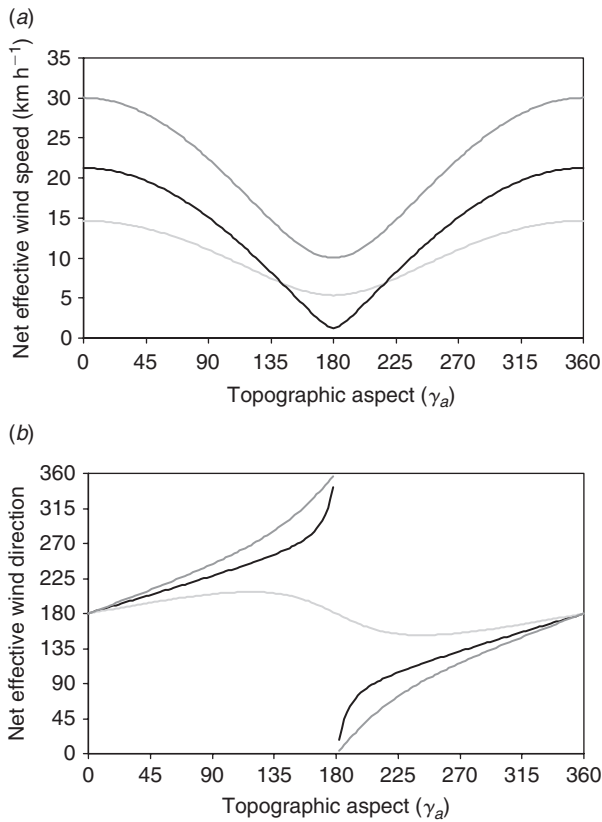


Fig. 5. (a) Net effective wind strength, and (b) net effective wind direction. The light grey, black and dark grey curves correspond to topographic slopes of 10°, 20° and 30°, respectively. The wind is assumed to be blowing at 10 km h⁻¹ from the north.

270°, the upslope component of the wind-induced rate of spread is zero and so scaling this makes no difference.

Methods such as the vector McArthur method may therefore be referred to as multiplicative whereas the McAlpine *et al.* approach may be referred to as additive. The multiplicative form of the McArthur method means that it does not admit the possibility of a fire burning upslope against the wind, as the approach of McAlpine *et al.* does.

McAlpine *et al.* (1991) point out that their method can be used to improve the Rothermel model (Eqn 9). The sum of the slope and wind factors $\phi_s + \phi_w$ present in Eqn 9 can be replaced (modulo some calibration terms) by $\mathbf{U}_{ws} = \mathbf{w} + \mathbf{w}_s^*$. As we have already seen in the method of Finney (1998), this effectively turns the scalar Rothermel method into a vector method. Some ambiguities arise in doing this, however. These ambiguities are discussed in the *General framework* section.

It is also interesting to point out that one could apply the logic of McAlpine *et al.* (1991) to the McArthur fire behaviour prediction framework. In this framework, the rate of spread is approximately given by (Noble *et al.* 1980)

$$\begin{aligned} R_w &= 1.5 \times 10^{-3} W_F D \exp\left(\frac{T-H}{30}\right) \exp(0.0234 \|\mathbf{w}\|) \\ &= R_0 \exp(0.0234 \|\mathbf{w}\|) \end{aligned} \quad (27)$$

Thus, assuming windless conditions and following the same reasoning as McAlpine *et al.* (1991), we can equate the right hand sides of Eqns 27 and 1 and obtain

$$\|\mathbf{w}_s^*\| = 2.96 \gamma_s \quad (28)$$

Hence the slope effect in the McArthur model can be mimicked by an equivalent upslope wind vector with magnitude given by Eqn 28.

Unfortunately, owing to the design of the McArthur model, Eqn 28 gives the equivalent wind speed in units of degrees! This means that we cannot add the upslope wind-equivalent vector to the ambient wind vector as done by McAlpine *et al.* This problem could be remedied by reformulating the slope correction Eqn 1 in terms of the slope ($\tan \gamma_s$) instead of the slope angle γ_s . Reformulating Eqn 1 as such admits the possibility of an *additive* McArthur method.

For the moment, let us assume that Eqn 23 is a suitable reformulation of Eqn 1. The close agreement of the two curves in Fig. 4 suggests that this is at least approximately so. Using Eqn 23 leads to an upslope wind equivalent given by

$$\|\mathbf{w}_s^*\| = 150.98 (\tan \gamma_s)^{1.2} \quad (29)$$

Hence, an *additive* vector McArthur approach results in a net effective wind vector given by

$$\begin{aligned} \mathbf{U}'_{ws} &= \|\mathbf{w}\| \sin(\theta_w - \gamma_s) \hat{\mathbf{t}} + (\|\mathbf{w}\| \cos(\theta_w - \gamma_s) \\ &\quad + 150.98 (\tan \gamma_s)^{1.2}) \hat{\mathbf{u}} \end{aligned} \quad (30)$$

Nelson

Elaborating on the ideas introduced in McAlpine *et al.* (1991) and Finney (1998), Nelson (2002) derives an effective wind speed that incorporates effects due to wind and slope by considering the effect of the motion of buoyant air upslope. The reasoning employed is in keeping with the intuitive notion that the extra heat flowing upslope will tend to 'steer' the fire in that direction. As mentioned, the main addition to this method is the inclusion of the vertical motion of air due to buoyancy, which is taken to have speed U_b . The component of this buoyant velocity parallel to the terrain surface at a given point is then given by $U_b \sin \gamma_s$.

In this method, an ambient wind vector \mathbf{w} is assumed to be blowing across a small segment of the head-fire. Working in terrain-following coordinates, the upslope component of the ambient wind is given by $\|\mathbf{w}\| \cos(\theta_w - \gamma_a)$ while the transverse component is given by $\|\mathbf{w}\| \sin(\theta_w - \gamma_a)$. Vectorially adding the upslope components of the ambient and buoyant wind motions to the transverse ambient wind component results in an effective wind vector

$$\mathbf{U}_{ws} = \|\mathbf{w}\| \sin(\theta_w - \gamma_a) \hat{\mathbf{t}} + (U_b \sin \gamma_s + \|\mathbf{w}\| \cos(\theta_w - \gamma_a)) \hat{\mathbf{u}} \quad (31)$$

with magnitude U_{ws} given by

$$U_{ws} = \sqrt{\|\mathbf{w}\|^2 \sin^2(\theta_w - \gamma_a) + (U_b \sin \gamma_s + \|\mathbf{w}\| \cos(\theta_w - \gamma_a))^2} \quad (32)$$

and direction θ_{ws} given by

$$\tan \theta_{ws} = \frac{\|\mathbf{w}\| \sin(\theta_w - \gamma_a)}{U_b \sin \gamma_s + \|\mathbf{w}\| \cos(\theta_w - \gamma_a)} \quad (33)$$

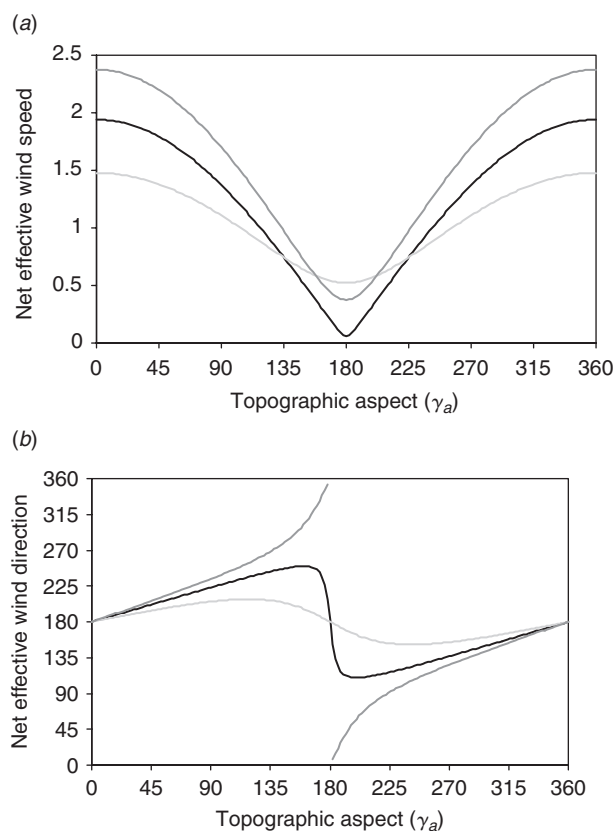


Fig. 6. (a) Magnitude of the slope-corrected effective wind speed U_{ws} ; (b) direction of the slope-corrected wind; the light grey, black and dark grey curves correspond to topographic slopes of 10° , 20° and 30° , respectively. A unit wind blowing from the north and a buoyant wind of 2.75 units have been assumed.

Note that some amendments will need to be made to Eqn 33 when $\theta_w - \gamma_a$ is greater than 90° . Some curves representing the general effective wind (and hence rate of spread) direction formula for three different slope angles are given in Fig. 6, alongside the corresponding curves depicting how the effective wind speed varies with topographic aspect. The curves were derived assuming that $U_b = 2.75$ as this vertical velocity gives rise to a flame angle of approximately 20° when the horizontal wind speed is taken as unity.

We again note that the effective wind direction curves display significantly different behaviour to that seen in Fig. 2b. The cusp points seen at aspect angles of 90° and 270° in Fig. 2b are not present in Fig. 6b, as was the case for the method of McAlpine *et al.* This is due to the fact that in Nelson's method, the upslope component of the buoyant wind velocity is *added* to the upslope component of the ambient wind, whereas in the McArthur methods the upslope component of the wind-based rate of spread vector is *multiplied* by a scaling factor. Nelson's method is another example of an additive vector method.

The curves in Fig. 6b display some interesting behaviour. For mild topographic slopes (10° , 20°), the effective wind direction tends to deviate towards the upslope direction for aspects between 0° and 180° but for a downslope fire ($\gamma_a = 180^\circ$), the

effective wind direction is downslope, which means that the fire will propagate as a downslope heading fire. However, for topographic slopes beyond some threshold value, the fire will tend to burn upslope against the ambient wind. This can be seen in the curve corresponding to $\gamma_s = 30^\circ$ in Fig. 6b. A formula for determining the threshold topographic slope is given in Nelson (2002): the sine of the threshold topographic slope angle γ_s^* is given as the ratio of the ambient and buoyant wind speeds, that is

$$\sin \gamma_s^* = \frac{\|\mathbf{w}\|}{U_b} \quad (34)$$

For the example portrayed in Fig. 6b, the threshold topographic slope angle is $\gamma_s^* \approx 21.3^\circ$.

McRae

McRae (2004a) proposed a simple geometric approach to describe the effect of slope on a fire's rate of spread. The approach invokes the concept of flame tilt angle and considers the relative advance of an upslope flame as compared with that of an identical flame in flat terrain. The flame tilt angle or simply the flame angle θ_f is defined as the angle that the front face of the flame makes with the vertical. Note that $\theta_f > 0$ for a heading fire (a fire whose flames lean over unburnt fuel) and $\theta_f < 0$ for a backing fire (a fire whose flames lean over burnt fuel). The flame angle results from a combination of the buoyant vertical motion of the (local) air due to heating and the horizontal motion of the air due to the prevailing winds. Hence, in windless conditions the flame angle will be zero (flame is vertical), as there is no horizontal component to the motion of the air. The inclusion of the flame angle, which depends on the buoyant vertical motion of air, means that this approach can be seen to be roughly analogous to the method of Nelson (2002). It should be pointed out, however, that this method assumes the ambient wind travels horizontally rather than parallel to the surface, as is assumed in Nelson's method.

The flame angle is important for the rate of spread of a wildfire propagating via radiative heat transfer. In the case of a heading fire, flames tilting towards unburnt fuel extend the range of radiative heat transfer (preheating range), which acts to increase the rate of spread, whereas for a backing fire, the range of heat transfer is decreased and the fire's rate of spread is consequently decreased (Pyne 1984).

The flame angle is also important for fires spreading by direct flame contact with adjacent fuels and it is this aspect that is best represented in the present approach. If we consider a heading fire burning in flat terrain, then we may take the rate of spread (due to flame contact) as proportional to the length a , the horizontal displacement of the flame at the height of the fuel, as depicted in Fig. 7a. If however, the terrain is inclined at an angle γ_s to the horizontal, so that the fire is propagating upslope, then the slope also contributes to the rate of spread. This situation is depicted in Fig. 7b.

As can be seen with reference to Fig. 7a and b, the horizontal displacement of the flame at the height of the fuel is now given by the length $c > a$. The contribution of topographic slope to the rate of spread of the fire is then described by the wind-corrected factor, which is estimated as the ratio $\Gamma = c/a$.

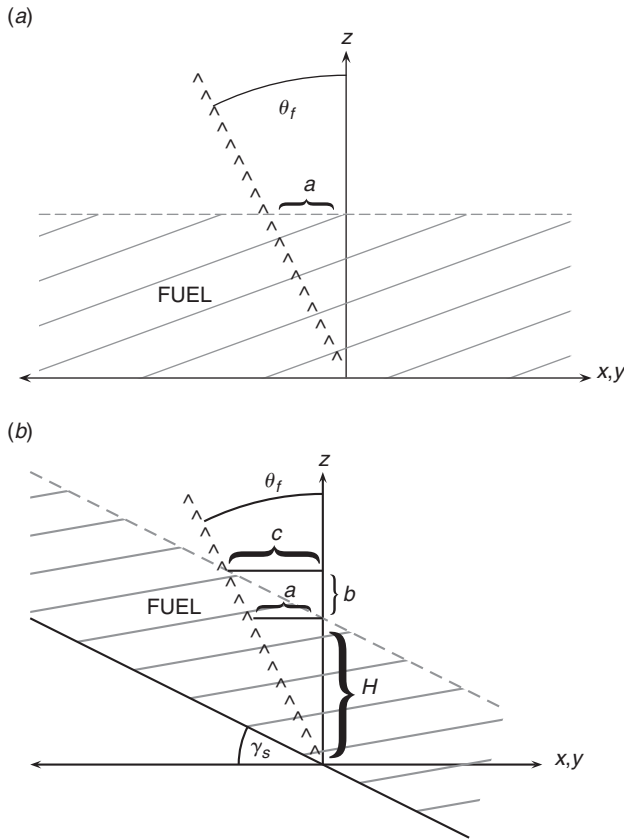


Fig. 7. Schematics showing how flames come into contact with fuel in (a) flat terrain, and (b) sloping terrain.

Working with the aid of Fig. 7a and b, we have:

$$\tan \gamma_s = \frac{b}{c}, \quad \text{and} \quad \tan \theta_f = \frac{c}{b + H} = \frac{a}{H}$$

hence,

$$\frac{c}{c \tan \gamma_s + H} = \frac{a}{H}$$

Rearranging, we obtain

$$\begin{aligned} \frac{c}{a} &= \frac{H}{H - a \tan \gamma_s} \\ &= \frac{H}{H - H \tan \theta_f \tan \gamma_s} \\ &= \frac{1}{1 - \tan \theta_f \tan \gamma_s} \end{aligned}$$

Hence the wind-slope correction factor is estimated as

$$\Gamma = (1 - \tan \theta_f \tan \gamma_s)^{-1} \quad (35)$$

So far we have considered the effect of wind and slope on a fire's rate of spread in the case when the prevailing wind and the topographic slope are aligned so that the wind is blowing directly upslope. As mentioned previously, this is hardly ever the case. To obtain an expression for the general situation, there

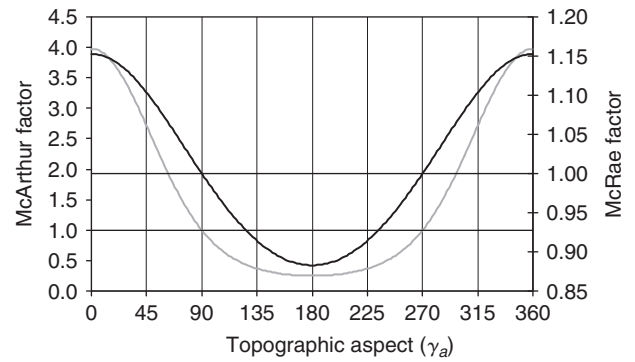


Fig. 8. Comparison of the slope-correction factors from the McArthur (black) and McRae (grey) methods. A topographic slope of 20° and a flame angle of 20° have been assumed.

are again two ways to proceed. As before, the scalar method involves deriving an amended topographic slope angle that is valid for all wind directions, whereas the vector method involves a vector decomposition of the wind-induced rate of spread vector before applying the above slope correction formula to the upslope component of the wind-induced rate of spread only.

Applying the scalar method, we need to replace the upslope gradient $\tan \gamma_s$ with the gradient experienced in the direction of the wind-induced rate of spread. This quantity was calculated in Eqn 4. Thus substituting $\tan \psi$ as given by Eqn 4 in place of $\tan \gamma_s$ in Eqn 35, we obtain an expression for the slope-correction factor as

$$\Gamma = (1 - \tan \theta_f \tan \gamma_s \cos(\theta_w - \gamma_a))^{-1} \quad (36)$$

Therefore the slope-corrected rate of spread, according to this method, is given by

$$R(w, \gamma_s) = \frac{R_w}{1 - \tan \theta_f \tan \gamma_s \cos(\theta_w - \gamma_a)} \quad (37)$$

Fig. 8 gives a comparison of the slope-correction factors derived using the McArthur relationship (Eqn 1) and the McRae relationship (Eqn 35). The curves in Fig. 8 are derived assuming that the wind is blowing from the north and that the topographic slope is 20°. The flame angle was taken to be 20°, regardless of the aspect. The assumption of a 20° flame angle simplifies the comparison but is perhaps not well justified for all aspects. An approach like that utilised in Nelson's method, where flame angle is derived based on buoyancy effects could lead to more realistic results but this possibility is not pursued here.

Fig. 8 illustrates that the slope-correction factors derived using the McArthur and McRae methods give rise to curves of similar shape. One would therefore expect that, once the various calibration constants have been taken into account, the two methods would give quantitatively similar predictions for the scalar rate of spread.

We can extend the scalar relationship (Eqn 37) to apply in a vector setting as was done in obtaining Eqn 6. This involves scaling the upslope component of the wind-induced rate of spread vector by the scaling factor in Eqn 37, only now the flame angle θ_f is replaced by the flame angle experienced in the upslope

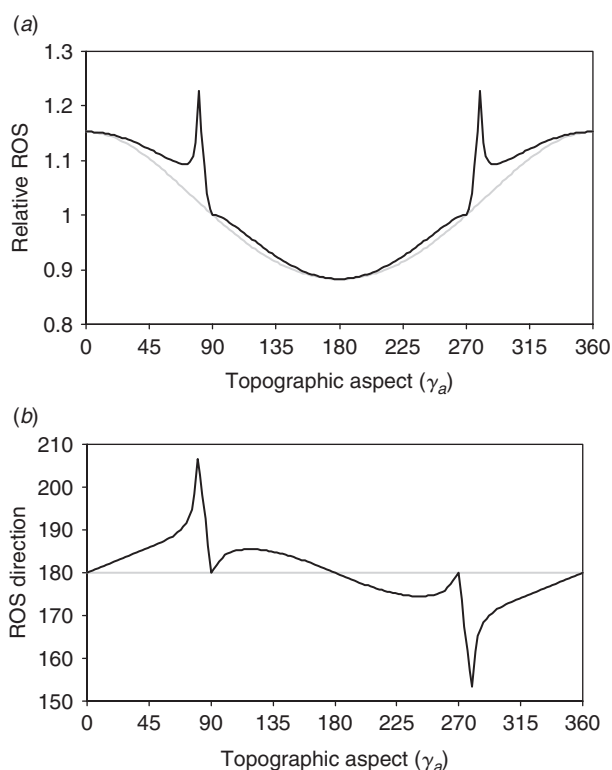


Fig. 9. (a) Magnitude of the slope-corrected rate of spread: the black line is derived using the vector method, whereas the grey line is derived using the scalar method; (b) direction of the slope-corrected rate of spread vector; the black line is derived using the vector method; the grey line indicates that the scalar method doesn't alter the direction of spread. A unit wind from the north, a topographic slope of 20° and a flame angle of 20° have been assumed.

direction. As flame angle is measured from the vertical, this is accomplished by replacing $\tan \theta_f$ with $\tan \theta_f \sec(\theta_w - \gamma_a)$. This gives rise to the vector relationship

$$\mathbf{R}(\mathbf{w}, \gamma_s) = R_w \sin(\theta_w - \gamma_a) \hat{\mathbf{t}} + \frac{R_w \cos(\theta_w - \gamma_a)}{1 - \tan \theta_f \tan \gamma_s \sec(\theta_w - \gamma_a)} \hat{\mathbf{n}} \quad (38)$$

Application of Eqn 38 requires some caution. For example, the upslope component has a singularity when $\tan \theta_f \sec(\theta_w - \gamma_a) = \cot \gamma_s$. However, this does not cause a problem because we also require that the flame angle sensed in the upslope direction be less than the complement of the topographic slope angle, otherwise the flames penetrate the terrain surface. Hence, we have the supplementary condition

$$\tan \theta_f \sec(\theta_w - \gamma_a) < \cot \gamma_s \quad (39)$$

Imposing this condition ensures that the upslope component in Eqn 38 remains non-singular. Note further that as $\tan \theta_f \sec(\theta_w - \gamma_a) \rightarrow \cot \gamma_s$, the flames tend to become parallel to the terrain surface – this leads to a blow-up in the rate of spread. This can be seen in Fig. 9a where the magnitudes of the slope-corrected rate of spread given by Eqns 37 and 38 are compared. The curves in this figure were derived assuming a unit wind blowing from the north and a topographic slope of 20° . As before,

to simplify the comparison, a flame angle of 20° was assumed regardless of aspect. A comparison of the direction of spread derived from the two methods is shown in Fig. 9b. The effect on the direction of spread as the flames tend to become parallel to the terrain surface can again be seen in Fig. 9b, with the predicted direction diverging wildly upslope at aspects close to 90° and 270° , when the wind-induced rate of spread is transverse to the slope. However, the reader is reminded that McRae's method is a mathematical idealisation used to correct the head-fire rate of spread only. In reality, the discontinuities in Fig. 9a, b are likely to not be as extreme, if they occur at all, owing to the curvature of the fire perimeter and the likely variation in flame angle.

McRae's approach does have one disadvantage. Eqn 37 cannot be used when $\theta_f = 0$ (i.e. under windless conditions). In fact, the derivation of Eqn 37 does not apply since $a = 0$ in this case (see Fig. 7) and so the ratio c/a is undefined. Substituting $\theta_f = 0$ into Eqn 37, we find that $\mathbf{R}(\gamma_s) = \mathbf{R}_0$, which is independent of any topographic slope that might be present. Despite this shortcoming, the agreement with McArthur's empirically based method suggests that this simple geometrical approach captures at least some of the processes involved in wind-slope interaction.

It is also of interest to note that McRae's approach results in a wind-slope correction factor in which the effects of wind and slope are not additive. This is in keeping with results of empirical studies also (e.g. Murphy 1963).

Pagni and Peterson

The physical model of Pagni and Peterson (1973) is derived from the principle of conservation of energy, applied to an inclined, one-dimensional, homogeneous, porous fuel bed. The ambient wind is taken to be flowing parallel to the inclined fuel bed. In this model, the heat transfer mechanisms considered are essentially radiation, convection and conduction. The combined effects of wind and slope are included only in the radiative portion of heat transfer, where they are described by the shape factor between the flame and surface element. The shape factor is a function of the angle between the flame and the normal to the fuel bed, which is given by

$$\Omega_{ws} = \gamma_s + \theta_f \quad (40)$$

Here θ_f is an empirically determined flame tilt angle given by

$$\tan \theta_f = \frac{1.4 \|\mathbf{w}\|}{\sqrt{gL}} \quad (41)$$

where L is the flame length and g is the gravitational acceleration at the surface. Again, this amounts to treating the wind and slope effects as independent, additive factors, at least for the radiative component of heat transfer.

The shape factor (Eqn 40) is then used to modify a flame radiation term of the form

$$\Pi_{RF} = \frac{\alpha L}{2l_F} (1 + \sin \Omega_{ws}) \quad (42)$$

which is then added to the wind-induced rate of spread. Here α is the absorptivity of the fuel, L is the flame length and l_F is the fuel depth. Note that in this model, wind is also used to modify the convective budget. When wind and topographic slope are not aligned, we would again need to replace γ_s with the slope angle sensed in the direction of interest.

Morandini *et al.*

In a series of recent articles, European scientists have proposed a two-dimensional model of fire spread across a fuel bed. The model is essentially a thermal balance that gives rise to a reaction-diffusion partial differential equation for the spatio-temporal temperature distribution over the fuel bed. The solution of this partial differential equation, subject to suitable boundary and initial conditions, yields a combustion wave. The basic model, formulated assuming conditions of no-wind and no-slope, is described in Balbi *et al.* (1999). The problem of generalising the basic model to accommodate the presence of topographic slope is dealt with in Santoni *et al.* (1999). In this treatment, a supplementary radiative term is introduced into the thermal balance to account for the heat radiated from the flame ahead and upslope of the fire front. This term is modelled, using the Stefan–Boltzmann law, as

$$Q_{R_{\text{sup}}} = P(\gamma_s) \cos \xi T^4 \quad (43)$$

where ξ is the angle between the direction of slope (∇h) and the unit outward normal to the fireline. In the context of the models discussed previously, the supplementary radiation term could be expressed as

$$Q_{R_{\text{sup}}} = P(\gamma_s) \cos(\theta_w - \gamma_a) T^4 \quad (44)$$

The function P is determined empirically.

A method for including the combined effects of wind and slope in this model has been proposed by Morandini *et al.* (2002). In this treatment, the slope angle γ_s seen in Eqn 44 is replaced with the flame tilt angle $\beta_{ws} = \theta_f + \gamma_s$ (note that in Morandini *et al.*, the flame tilt angle is denoted by β_w and is referred to as the wind tilt angle, which is the flame tilt angle due to wind alone). Recall that in the absence of wind, the flame tilt angle reduces to the topographic slope angle because flames are supposed to be oriented vertically. Conversely, under wind and no-slope conditions, the flame tilt angle results from a balance between the (horizontal) wind and the buoyant vertical motion of the air. If the upward gas flow velocity is U_b , then the flame tilt angle under conditions of wind and no-slope is given by $\beta_{ws} = \theta_f$ where

$$\tan \theta_f = \frac{\|\mathbf{w}\|}{U_b} \quad (45)$$

Under conditions of wind and slope, there is a degree of ambiguity surrounding the calculation of flame tilt angle. The result of the calculation depends on whether we take the wind as horizontal or as parallel to the inclined surface. Taking the wind as flowing parallel to the inclined surface, we decompose the wind vector \mathbf{w} into its horizontal component $\|\mathbf{w}\| \cos \gamma_s$ and its vertical component $\|\mathbf{w}\| \sin \gamma_s$. These components can then be added (vectorially) to the upward gas flow velocity U_b to produce a wind tilt angle given by

$$\tan \theta_f = \frac{\|\mathbf{w}\| \cos \gamma_s}{U_b + \|\mathbf{w}\| \sin \gamma_s} \quad (46)$$

If, however, we take the wind as horizontal, then the upslope component of the wind vector is given by $\|\mathbf{w}\| \cos \gamma_s$. The upslope component of the wind vector may be further decomposed

into horizontal and vertical components given by $\|\mathbf{w}\| \cos^2 \gamma_s$ and $\|\mathbf{w}\| \cos \gamma_s \sin \gamma_s$, respectively. Hence, ignoring the component of wind perpendicular to the inclined surface, we obtain the following expression for the wind tilt angle

$$\tan \theta_f = \frac{\|\mathbf{w}\| \cos^2 \gamma_s}{U_b + \|\mathbf{w}\| \cos \gamma_s \sin \gamma_s} \quad (47)$$

Inclusion of the component of wind perpendicular to the inclined surface in the calculation of Eqn 47 results in Eqn 45.

To properly apply this method in operational situations, it is important to note how the wind is measured. Typically an anemometer is oriented so that it measures the horizontal component of the wind. When this is the case, Eqn 47 is likely to be more reliable than Eqn 46 that appears in Morandini *et al.* (2002). On average however, the wind is likely to be aligned more or less parallel to the terrain surface, except at locations where slope changes dramatically. Wind is also taken as parallel to the surface in transport models that estimate spatially varying wind fields over complex terrain (Forthofer *et al.* 2003; Butler *et al.* 2006). In reality, however, distinguishing when the wind should be taken as horizontal or parallel to the surface may be beyond the reasonable limits of operational accuracy.

To extend the approach of Morandini *et al.* to the more general setting, when the wind vector and topographic aspect are not aligned, one would need to replace slope and wind tilt angles by the corresponding angles sensed in the particular direction of interest, as was done in the *McRae* section.

A general framework

In this section, we discuss the formal similarities between the wind–slope correction methods of the various models discussed above.

The scalar methods fall into one of two classes. Members of the first class are characterised as being based on the wind-induced rate of spread and are of the form

$$R(\mathbf{w}, \gamma_s) = \sigma(\gamma_s, \theta_w, \gamma_a) R_w \quad (48)$$

In methods belonging to this class, the wind-induced rate of spread is multiplied by a slope correction factor to give a slope-corrected rate of spread. They may therefore be classed as multiplicative scalar methods.

Members of the second class are characterised as being based on the base rate of spread and may be expressed in the form

$$R(\mathbf{w}, \gamma_s) = (1 + \phi_{ws}(\|\mathbf{w}\|, \theta_w, \gamma_s, \gamma_a)) R_0 \quad (49)$$

In this class of methods, the base rate of spread is added to a term representing the rate of spread contribution due to wind and slope effects, where this term is modelled as a multiple of the base rate of spread. They can therefore be classed as additive scalar methods.

As we have seen, the scalar methods give rise to vector methods. Scalar methods of the form of Eqn 48 are readily generalised to vector methods that utilise the wind-based rate of spread vector. Doing so gives rise to following general framework

$$\mathbf{R}(\mathbf{w}, \gamma_s) = B_{-\gamma_a} S_{\gamma_s} B_{\gamma_a} \mathbf{R}_w \quad (50)$$

where B_{γ_a} is the change of basis matrix (Anton 1987), which facilitates a switch from the standard cardinal coordinates to the terrain-following coordinates,

$$B_{\gamma_a} = \begin{bmatrix} -\cos \gamma_a & \sin \gamma_a \\ -\sin \gamma_a & -\cos \gamma_a \end{bmatrix}$$

and S_{γ_s} is the slope-correction matrix given by

$$S_{\gamma_s} = \begin{bmatrix} 1 & 0 \\ 0 & \sigma \end{bmatrix}$$

Here σ is the same quantity given in Eqn 48, with the arguments omitted.

Eqn 50 spells out the steps involved in methods belonging to this class. First a coordinate transformation is applied so that we are working with respect to coordinate axes that are aligned with the upslope and transverse directions (B_{γ_a}); second, the scalar slope-correction relationship is applied to the upslope component of the wind-induced rate of spread vector (S_{γ_s}), and finally the coordinates are back-transformed so that the coordinate axes again align with the cardinal directions ($B_{-\gamma_a}$). Methods adhering to this form can be classed as multiplicative vector methods.

When one considers how the scalar methods of the form of Eqn 49 might be extended to a vector form, certain ambiguities arise. Both McAlpine *et al.* (1991) and Nelson (2002) assert that rate of spread models of the form of Eqn 49 could be improved by replacing ϕ_{ws} with an equivalent wind vector, derived as the sum of the ambient wind vector and an upslope wind-equivalent vector. Eqn 49, however, requires that the base rate of spread is scaled by the factor $1 + \phi_{ws}$, and so at least two options would seem to arise. The first option is to simply take the magnitude of the equivalent wind vector as the factor ϕ_{ws} , calculate the magnitude of the rate of spread using Eqn 49 and dictate that the direction of the wind-slope corrected rate of spread is simply that of the equivalent wind vector, so that

$$\begin{aligned} \|\mathbf{R}(\mathbf{w}, \gamma_s)\| &= (1 + \|\mathbf{U}_{ws}\|)R_0 \\ \theta_{\mathbf{R}} &= \theta_{ws} \end{aligned} \quad (51)$$

This is the method that seems to be advocated in McAlpine *et al.* (1991) and Nelson (2002).

The second option, which is perhaps the more natural one, is to assign a direction to the base rate of spread. We thus assume that the base rate of spread can be represented by a vector with length R_0 , directed along the outward normal to the fire front (as this is the direction one would expect the fire to propagate in the absence of wind and slope effects). This assumption then gives rise to the following general framework

$$\mathbf{R}(\mathbf{w}, \gamma_s) = (\hat{\mathbf{n}} + \mathbf{U}_{ws})R_0 \quad (52)$$

where $\hat{\mathbf{n}}$ denotes the unit outward normal at the particular point on the head-fire line. Rather than only ‘vectorising’ the factor ϕ_{ws} we have ‘vectorised’ the sum $1 + \phi_{ws}$. In this context, Eqn 51 can be seen as an approximate version of Eqn 52 that applies when the effects of wind and slope are the dominant fire-spread mechanisms, i.e. when $\|\mathbf{U}_{ws}\| \gg 1$. Methods that adhere to this form may be classed as additive vector methods.

The outward unit normal to the fire perimeter also naturally arises when one considers how to apply wind-slope correction to the whole fire perimeter. For example, in the additive vector method espoused by Viegas (2004a), the outward unit normal to the fire perimeter can be used to section the fire perimeter into parts corresponding to different spread directions. In this approach, the slope effect is again represented by a vector directed upslope, which is added to the wind-induced rate of spread vector. However, for different parts of the fire perimeter, the slope and wind effects can be parallel or antiparallel to the slope and wind directions, depending on whether $\nabla h \cdot \hat{\mathbf{n}}$ and $\mathbf{w} \cdot \hat{\mathbf{n}}$ are positive or negative. Wind-slope correction methods applicable to the whole fire perimeter, such as that discussed in Viegas (2004a), are of major importance for understanding landscape-scale fires in complex terrain where the concept of ‘head-fire’ is not always well defined.

Discussion

We have presented a range of methods used to correct fire rate of spread for the effects of wind and topographic slope. The methods were based on either empirical knowledge of the response of the rate of spread of a fire to wind and topographic slope, on geometric reasoning, or on a combination of the two. Both scalar and vector methods for wind-slope correction have been discussed. The vector methods tended to give more realistic results than the scalar methods – this is particularly true of the predicted direction of spread. The scalar methods do not allow for the fact that the effects of wind and slope are directional. However, the vector methods take into account the alignment of the wind and slope effects. Vector methods treat the slope effect as being directed upslope as this fits with our intuition that the extra heat moving upslope tends to steer the fire in that direction.

The vector formulation of the empirically based approach of McArthur discussed above produces reasonable results except when the wind-induced rate of spread is aligned across a slope. The method predicts that in these instances topographic slope does not affect the direction of spread; a fire will continue to burn across slope regardless of the gradient of the terrain. This is at odds with observations of actual fires that have an upslope component to their propagation even when the wind, and hence the wind-induced rate of spread, are directed in a direction perpendicular to the upslope direction. The reason for this shortcoming lies in the multiplicative form of the method. This problem could be overcome by reformulating McArthur’s approach as an additive vector method, in the spirit of the approach of McAlpine *et al.* (1991) and Finney (1998).

The approach of McRae, which also has a multiplicative form, suffers from the same problem as the McArthur approach and has the additional shortcoming of not accounting for slope effects in the absence of wind. The geometrical approach of McRae, however, is appealing because it is formulated using basic mathematical principles and results in a function of quite similar shape to those derived empirically. It is therefore likely that such a formulation could be calibrated so as to apply to any particular location or fuel type. It is also interesting to note that this simple geometric approach leads to a function that is not additive with respect to wind and slope effects, a property that is assumed in

methods such as that of Rothermel (1972), Pagni and Peterson (1973) and Morandini *et al.* (2002).

The approach of Rothermel and Albini is an extension of Rothermel's scalar method that takes account of the direction of wind and slope in a limited way, without progressing to a full vector form of the model. This additive approach was able to capture some of the features contained in the vector multiplicative McArthur approach. Again this serves to demonstrate the strength of an additive approach to wind–slope correction of head-fire rates of spread. The additive vector approach of Finney (1998) extends the method to a full vector approach, thereby overcoming some of the shortcomings of the scalar approach.

The additive vector method of McAlpine *et al.* (1991) assumes that the effect of topographic slope can be approximated by an equivalent upslope wind field. Such an approach again fits with our intuition that topographic slope tends to steer a fire in the upslope direction. However, as pointed out by McAlpine (pers. comm., 2006), the non-linear nature of fire spread models means that care needs to be taken in the application and interpretation of these types of methods. Using vector addition to combine the individual rates of spread due to slope and wind will give a different predicted net rate of spread vector than would be obtained by first adding the wind and upslope wind-equivalent vectors and using the resultant net wind vector to predict the rate of spread vector.

A disadvantage of the approach of McAlpine *et al.* (1991) is that it breaks down for large topographic slopes (see Eqn 26). This reflects the fact that empirical studies at both laboratory and field scales typically consider slopes under 50°. However, because slopes steeper than 50° can sometimes occur in the landscape, it would seem reasonable to desire a model that can accommodate such occurrences.

The approach of McAlpine *et al.* also admits the possibility of a fire burning upslope against the wind. Although this sort of fire behaviour might be atypical, actual fires have been observed to display this sort of behaviour. It would therefore seem reasonable to favour methods that can accommodate this possibility.

The approach of Nelson, another additive vector method, uses the buoyant motion of the air caused by the heat of the fire to define an equivalent upslope wind field to account for the effect of topographic slope. As such, this approach captures some of the actual processes involved in the modulation of fire spread by slope effects. Another advantage is that it accommodates the possibility of a fire burning upslope against the ambient winds. In terms of the processes underlying Nelson's approach, this type of behaviour can be expected when the buoyant motion of the air generated by the heat of the fire dominates the ambient motion of the air. A disadvantage of the approach is that it is circular: the equivalent upslope wind due to buoyancy is defined in terms of the rate of spread (via Byram's intensity, Byram (1959)), which according to the approach, is obtained from the equivalent upslope wind. This means that the approach must be applied iteratively. However, although this might be a disadvantage from the computational point of view, the intent of the method is to capture the coupling between heat transfer and the buoyancy-induced flow, first proposed for upslope fires in the absence of wind by Dupuy and Larini (1999).

The methods of Pagni and Peterson and Morandini *et al.* both treat wind and slope effects as non-directional, independent,

additive factors. In essence, these two wind–slope correction methods are scalar methods. Pagni and Peterson's approach is manifestly one-dimensional and so doesn't account for the directional effects of wind and slope. The method of Morandini *et al.* is intended for use as part of a two-dimensional dynamical system based on conservation of energy requirements. It therefore seems likely, provided that the directional effects of wind and slope are accounted for, that the approach of Morandini *et al.* could reproduce some of the behaviour predicted by approaches such as those of McAlpine *et al.* and Nelson. One point of ambiguity surrounding the approach of Morandini *et al.* concerns the notion of wind vector. In this method, different results were derived depending on whether the wind field was taken as being directed horizontally or parallel to the terrain surface. Ideally there should be a convention about which wind vector is the one for standardised use, though this may exceed what can be expected of current operational data-gathering procedures. From a geometric point of view, adopting a convention that takes the wind vector as flowing parallel to the terrain surface is perhaps more appealing as this naturally enables the concept of wind vector at a point to be extended to that of a wind vector-field defined on the terrain surface. Given that the terrain surface is represented by a differentiable manifold M (Abraham *et al.* 1988), such a wind vector field belongs to the tangent bundle TM , which is the collection of all vectors that are parallel to the surface M . The tangent bundle would play a canonical role in any geometric modelling considerations. Adopting a convention that takes wind as flowing parallel to the surface is also in keeping with the fact the mean wind is likely to be parallel to the terrain surface, except at places where slope changes rapidly, and the fact that transport models for estimating spatially varying wind fields produce outputs that are parallel to the terrain surface. However, anemometers are usually aligned horizontally, so that from the operational point of view, models assuming a horizontal wind field are more immediately appealing.

Overall, the additive vector methods tended to best represent the vectorial nature of wind and slope effects, giving the most realistic and intuitively reasonable results. It would also seem that additive vector approaches are more naturally extendable to wind–slope correction methods that apply to the whole fire perimeter. It should be noted that although the inclusion of wind and slope correction methods can extend the predictive capability of point-functional models of fire spread, it does not necessarily overcome all of their limitations. Dynamic feedback effects (Viegas 2002, 2004a, 2004b, 2006; Viegas and Pita 2004; Oliveras *et al.* 2006) and coupling between the fire, the topography and the atmosphere (Linn *et al.* 2007) can produce fire behaviour that may not be accounted for by point-functional models. Further experimentation with laboratory fires, careful analysis of actual bushfires incorporating wind and terrain characteristics and numerical simulation of wind- and slope-driven fires with fully coupled fire–topography–atmosphere models are all required to evaluate and refine the wind–slope correction methods discussed in the present paper.

Acknowledgements

The author would like to thank G. Mills, R. McAlpine and J. S. Gould for their comments on a draft version of the present manuscript. Thanks are also due to D. X. Viegas, M. Alexander and F. Morandini for their helpful and

friendly correspondence on this topic, and R. McRae, R. Weber, K. Tolhurst and D. Chong for illuminating discussions concerning wind–slope correction of fire rate of spread. The author also gratefully acknowledges the support of the Bushfire CRC and the anonymous reviewers whose suggestions helped broaden the context of the paper.

References

- Abraham R, Marsden JE, Ratiu T (1988) 'Manifolds, Tensor Analysis and Applications.' 2nd edn. (Springer-Verlag: New York)
- Albini FA (1976) Combining wind and slope effects on spread rate. Unpublished memo to RC Rothermel dated 19/1/76. On file at Intermountain Fire Sciences Lab. (Missoula, MT)
- Anton H (1987) 'Elementary Linear Algebra.' 5th edn. (Wiley: New York)
- Balbi JH, Santoni PA, Dupuy JL (1999) Dynamic modelling of fire spread across a fuel bed. *International Journal of Wildland Fire* **9**, 275–284. doi:10.1071/WF00005
- Beck JA (1990) Equations for the forest fire behaviour tables for Western Australia. *CALM Science* **1**(3), 325–348.
- Beer T (1991) Bushfire rate of spread forecasting: deterministic and statistical approaches to fire modeling. *Journal of Forecasting* **10**, 301–317. doi:10.1002/FOR.3980100306
- Butler BW, Bartlette RA, Bradshaw LS, Cohen JD, Andrews P, Putnam T, Mangan RJ, Brown H (1998) Fire Behavior Associated with the 1994 South Canyon Fire on Storm King Mountain, Colorado. USDA Forest Service, Rocky Mountain Research Station, Research Paper RMRMS-RP-9. (Ogden, UT)
- Butler BW, Bartlette RA, Bradshaw LS, Cohen JD, Andrews PL, Putnam T, Mangan RJ, Brown H (2003) The South Canyon Fire revisited: lessons in fire behaviour. *Fire Management Today* **63**(4), 77–84.
- Butler BW, Forthofer JM, Finney MA, McHugh C, Stratton R, Bradshaw LS (2006) The impact of high-resolution wind field simulations on the accuracy of fire growth predictions. In 'Proceedings of the 5th International Conference on Forest Fire Research'. 27–30 November 2006, Figueira da Foz, Portugal. (Ed. DX Viegas) (Elsevier B.V.: Amsterdam)
- Byram GM (1959) Forest fire behaviour. In 'Forest Fire: Control and Use'. (Ed. KP Davis) (McGraw-Hill: New York)
- Byram GM, Clements HB, Bishop ME, Nelson RM, Jr (1966) Final report – PROJECT FIRE MODEL: an explanatory study of model fires. Office of Civil Defense Contract OCD-PS-65–40, USDA Forest Service, Southeastern Forest Experiment Station. (Asheville, NC)
- Dold J, Weber R, Gill AM, Ellis P, McRae R, Cooper N (2005) Unusual phenomena in an extreme bushfire. In 'Proceedings of the 5th Asia-Pacific Conference on Combustion', 17–20 July 2005, The University of Adelaide, South Australia. (Ed. K King) (University of Adelaide: Adelaide)
- Dupuy J-L, Larini M (1999) Fire spread through a porous forest fuel bed: a radiative and convective model including fire-induced flow effects. *International Journal of Wildland Fire* **9**(3), 155–172. doi:10.1071/WF00006
- Finney MA (1998) FARSITE: Fire Area Simulator – model development and application. USDA Forest Service, Rocky Mountain Research Station Research Paper RMRS-RP-4. (Ogden, UT)
- Fons WL (1946) Analysis of fire spread in light forest fuels. *Journal of Agricultural Research* **54**(4), 239–267.
- Forestry Canada Fire Danger Group (1992) Development and structure of the Canadian Forest Fire Behavior Prediction System. Forestry Canada, Science and Sustainable Development Directorate, Information Report ST-X-3. (Ottawa, ON)
- Forthofer JM, Butler BW, Shannon KS, Finney MA, Bradshaw LS, Stratton R (2003) Predicting surface winds in complex terrain for use in fire spread models. In 'Proceedings of the 5th Symposium on Fire and Forest Meteorology', November 2003, Orlando, FL. (American Meteorological Society: Boston, MA)
- Linn RR (1997) Transport model for prediction of wildfire behaviour. Los Alamos National Laboratory, Scientific Report LA13334-T. (Los Alamos, NM)
- Linn RR, Winterkamp J, Edminster C, Colman JJ, Smith WS (2007) Coupled influences of topography and wind on wildland fire behaviour. *International Journal of Wildland Fire* **16**, 183–195. doi:10.1071/WF06078
- McAlpine RS, Lawson BD, Taylor E (1991) Fire spread across a slope. In 'Proceedings, 11th Conference on Fire and Forest Meteorology', 16–19 April 1991, Missoula, MT. (Ed. DF Potts) pp. 218–225. (Society of American Foresters: Bethesda, MD)
- McArthur AG (1966) Weather and grassland fire behaviour. Department of National Development, Forestry and Timber Bureau Leaflet No. 100. (Canberra, ACT)
- McArthur AG (1967) Fire behaviour in eucalypt forests. Department of National Development, Forestry and Timber Bureau Leaflet No. 107. (Canberra, ACT)
- McCarthy MA, Cary GJ (2002) Fire regimes in landscapes: models and realities. In 'Flammable Australia'. (Eds RA Bradstock, JE Williams, AM Gill) (Cambridge University Press: New York)
- McRae R (2004a) Virtually volvelles. In 'Proceedings, Bushfire 2004', May 2004, Adelaide, SA. (Department of Environment and Heritage, South Australia: Adelaide, SA)
- McRae R (2004b) Breath of the dragon – observations of the January 2003 ACT Bushfires. In 'Proceedings, Bushfire 2004', May 2004, Adelaide, SA. (Department of Environment and Heritage, South Australia: Adelaide, SA)
- McRae R, Weber RO, Sharples JJ (2006) Lessons from the 2003 fires – advancing bushfire risk management in the high country. In 'Proceedings, Bushfire 2006', June 2006, Brisbane, QLD. (Ed. C Tran) (Griffith University: Brisbane, QLD)
- Morandini F, Santoni PA, Balbi JH, Ventura JM, Mendes-Lopes JM (2002) A two-dimensional model of fire spread across a fuel bed including wind combined with slope conditions. *International Journal of Wildland Fire* **11**, 53–64. doi:10.1071/WF01043
- Murphy PJ (1963) Rate of fire spread in an artificial fuel. MS Thesis, Montana State University, Bozeman, MT.
- Nelson RM, Jr (2002) An effective wind speed for models of fire spread. *International Journal of Wildland Fire* **11**, 153–161. doi:10.1071/WF02031
- Noble IR, Bary GAV, Gill AM (1980) McArthur's fire-danger meters expressed as equations. *Australian Journal of Ecology* **5**, 201–203. doi:10.1111/J.1442-9993.1980.TB01243.X
- Oliveras I, Piñol J, Viegas DX (2006) Generalisation of the fire line rotation model to curved fire lines. *International Journal of Wildland Fire* **15**, 447–456. doi:10.1071/WF05046
- Rothermel RC (1972) A mathematical model for predicting fire spread in wildland fuels. USDA Forest Service, Intermountain Research Station, Research Paper INT-115. (Ogden, UT)
- Rothermel RC (1993) Mann Gulch Fire: a race that couldn't be won. USDA Forest Service, Intermountain Research Station General Technical Report INT-299. (Ogden, UT)
- Rothermel RC, Mutch RW (1986) Behaviour of the life-threatening Butte Fire: August 27–29, 1985. *Fire Management Notes* **47**(2), 14–24.
- Pagni PJ, Peterson TG (1973) Flame spread through porous fuels. In 'Fourteenth International Symposium on Combustion', Pittsburgh, PA. pp. 1099–1106. (The Combustion Inst.: Pittsburgh, PA)
- Pyne SJ (1984) 'Introduction to Wildland Fire.' (Wiley: New York)
- Santoni PA, Balbi JH, Dupuy JL (1999) Dynamic modelling of upslope fire growth. *International Journal of Wildland Fire* **9**, 285–292. doi:10.1071/WF00004
- Sneeuwjagt RJ, Peet GB (1985) 'Forest Fire Behaviour Tables for Western Australia.' 3rd edn. (Department of Conservation and Land Management: Perth, WA)

- Stewart J (1991) 'Calculus.' (Brooks-Cole Publishing: Belmont, CA)
- Van Wagner CE (1977) Effect of slope on fire spread rate. *Canadian Forestry Service Bi-monthly Research Notes* **33**, 7–8.
- Van Wagner CE, Pickett TL (1975) Equations and FORTRAN IV program for the 1976 metric version of the forest fire weather index. Environment Canada, Forestry Service Information Report PS-X-58. (Chalk River, ON)
- Viegas DX (2002) Fire line rotation as a mechanism for fire spread on a uniform slope. *International Journal of Wildland Fire* **11**, 11–23. doi:10.1071/WF01049
- Viegas DX (2004a) Slope and wind effects on fire propagation. *International Journal of Wildland Fire* **13**, 143–156. doi:10.1071/WF03046
- Viegas DX (2004b) A mathematical model for forest fires blow-up. *Combustion Science and Technology* **177**, 27–51. doi:10.1080/00102200590883624
- Viegas DX (2006) Parametric study of an eruptive fire behaviour model. *International Journal of Wildland Fire* **15**, 169–177. doi:10.1071/WF05050
- Viegas DX, Pita LP (2004) Fire spread in canyons. *International Journal of Wildland Fire* **13**, 253–274. doi:10.1071/WF03050
- Weber RO (2001) Wildland fire spread models. In 'Forest Fires. Behavior and Ecological Effects'. (Eds EA Johnson, K Miyanishi) pp. 151–169. (Academic Press: San Diego, CA)
- Weise DR (1993) Modelling wind and slope-induced wildland fire behaviour. PhD Thesis, University of California, Berkeley.
- Weise DR, Biging GS (1997) A qualitative comparison of fire spread models incorporating wind and slope effects. *Forest Science* **43**, 170–180.

Manuscript received 11 November 2006, accepted 18 October 2007